Electronic Supplementary Material (ESI) for Nanoscale.
This journal is © The Royal Society of Chemistry 2018

Characterizing Percolative Materials by Straining

Heming Yao[1], Marek Hempel[2], Jing Kong[2], Ya-Ping Hsieh[3], and Mario Hofmann[4]*

Heming Yao,
1. Department of Electrical and Electronic Engineering, The University of Hong Kong, Hong Kong

Marek Hempel
2. Department of Electrical Engineering and Computer Science, Massachusetts Institute of Technology, Cambridge, USA

Prof. Jing Kong
2. Department of Electrical Engineering and Computer Science, Massachusetts Institute of Technology, Cambridge, USA

Prof. Ya-Ping Hsieh
3. Institute for Atomic and Molecular Sciences, Academia Sinica, Taipei, Taiwan

Prof. Mario Hofmann
4. Department of Physics, National Taiwan University, Taipei, Taiwan
*Mario@phys.ntu.edu.tw

Supplementary Information:

I) Deformation of Percolative Film

For a percolative film, conducting nanopieces are randomly deposited on the substrate area and the conductivity follows the aforementioned percolation law.[1-6] The thickness t of percolative film is often used to demonstrate its percolation property,[2, 3, 5-7] and it follows $t \propto N_A$, where N_A is the number density of the film, meaning the number of nanopieces per unit area. Thus, with a certain number of nanopieces in the percolative film, the cross-section of the percolative film controls the number density N_A and the thickness t. Different from bulk films, uniaxial strain ε will change the position of the percolative film's constituents while retaining their shape. Under these conditions, strain will change the percolation conditions significantly since critical pathways may be broken.

To model this behaviour, we consider the changes to the sample area. Upon straining there is an elongation

$$L(\varepsilon) = L_0(1+\varepsilon) \tag{S1}$$

If the material (or the substrate) has an appreciable Poisson ratio μ, the width is also affected by strain.

$$W(\varepsilon) = W_0(1-\mu\varepsilon) \tag{S2}$$

To extract the thickness of the film under strain, we have to account for the discrete nature of the conductive links where neighboring constituents cannot occupy the same volume. We accomplish this task by assuming a fixed equivalent volume for each constituent that doesn't change with strain (which is justified by the observation that the matrix is usually much softer than the conductive links). In this case the conductive links would not be deformed by strain but reorganize within the strained matrix.[2] Strain induced changes to the matrix's area would thus result in a decreasing number density of constituents in out-of-plane direction, yielding the change of film thickness.

$$t(\varepsilon) = t_0/(1+\varepsilon)\,(1-\mu\varepsilon) \tag{S3}$$

where t_0, L_0, W_0 are the original film thickness, length and width, ($t(\varepsilon=0)$, $L(\varepsilon=0)$, $W(\varepsilon=0)$, respectively).

We thus find that the application of strain to a sample has the same effect as changing its thickness.

II) Resistance of Percolative Film

Previous work has determined the conductivity of percolative films to follow[2, 3, 5, 7, 8]:

$$\sigma_{DC,perc} = \sigma_{DC,bulk}\left(\frac{t-t_c}{t_{min}-t_c}\right)^n \tag{S4}$$

It can be seen that below a critical thickness (t_c) no conduction occurs, because the film fails to form an interconnected network[2, 3, 5]. Moreover, the percolation conductivity $\sigma_{DC,perc}$ approaches the bulk conductivity $\sigma_{DC,bulk}$ if the film thickness reaches t_{min} and yields unphysical values for $t>t_{min}$.

The sheet resistance of the percolative film can be expressed as equation (S5).

$$R_S = (\sigma_{DC,perc} t)^{-1} \tag{S5}$$

Using Equation (S1), the resistance of percolative film is:

$$R = \left(\frac{L}{W}\right)(\sigma_{DC,perc} t)^{-1} = \left(\frac{L}{W}\right)\left(\sigma_{DC,bulk}\left(\frac{t - t_c}{t_{min} - t_c}\right)^n t\right)^{-1} = \frac{L(t_{min} - t_c)^n}{W\sigma_{DC,bulk} {t_c}^{n+1}}\left(\frac{t_c}{t - t_c}\right)^n \frac{t_c}{t} \tag{S6}$$

Based on equation (S1)-(S3) and (S6), the resistance of a percolative film is modified by strain according to the equation (S7)

$$R(\varepsilon) = \frac{L(\varepsilon)(t_{min} - t_c)^n}{W(\varepsilon)\sigma_{DC,bulk} {t_c}^{n+1}}\left(\frac{t_c}{t(\varepsilon) - t_c}\right)^n \frac{t_c}{t(\varepsilon)} \tag{S7}$$

To make the equation applicable to experimental confirmation (S7), we normalize the resistance to the initial resistance to obtain equation (S8)

$$R(\varepsilon)/R(0) = \left(\frac{t_0 - t_c}{t(\varepsilon) - t_c}\right)^n (1 + \varepsilon)^2 \tag{S8}$$

Where $t(\varepsilon) = t_0/(1 + \varepsilon)\,(1 - \mu\varepsilon)$ is obtained from equation (S3).

III) Flake Films By Spray Deposition

The multi-sample measurements of graphene flake films are produced by spray deposition on polyethylene terephthalate (PET).[9, 10] A spraying gun was used to uniformly spray the solution onto PET substrates, under which there is the laterally movable heater. The sample was kept at elevated temperature and a surface temperature of 130°C was chosen to avoid degrading the polymer substrate. A typical spray process took about 20 minutes. The volume of sprayed graphene solution usually ranged from 3-7 ml for an area of 10 mm x 20 mm.

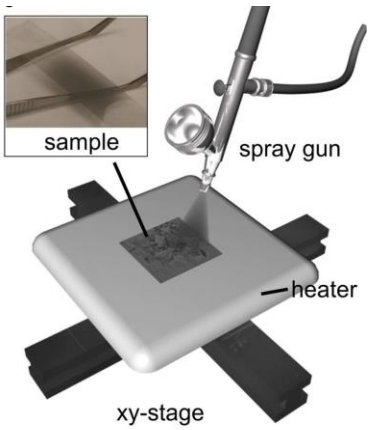

Figure S1. Schematic of experimental device and sample.

IV) Overview of characterized samples

	Material	Details	Reference
Figure 3(a)	Nickel-filled and Cu-Filled Polydimethylsiloxane (PDMS)	Cu nanostars and Ni nanoparticles were dispersed in ethanol and blended with PDMS copolymer by ultrasonication. The weight ratio was 3:1 for the PDMS-Ni and 2:1 for PDMS-Cu.	[11]
Figure 3(b)	Graphite nanosheets (GNs) and silicone rubber (SR) composites	GNs were mixed with Room-temperature vulcanized (RTV) liquid silicone rubber to form electrically conductive polymer nanocomposite, with a volume ratio of 1.36 vol %.	[12, 13]
Figure 4(b)	Multi-walled carbon nanotubes (MWNTs) and poly(methyl methacrylate) (PMMA) polymer composites	MWNTs and polymer pellets were dissolved in a solvent and mixed using ultrasound. The solvent was subsequently removed by air-dry to produce polymer/MWNT composites having different weight fractions.	[14]
Figure 4(c)	Ag/silica nanocomposite sol–gel films	Ag/silica nanocomposite is fabricated using an ultra-violet (UV) photo-reduction process, and is studied over a large range of Ag volume fractions.	[15]
Figure 4(d)	solution processed graphene flakes films	The graphene solution was produced by expansion of graphite flakes through microwave irradiation and subsequent mechanical exfoliation by sonication in 1-methylpyrrolidone (NMP) solvent. The film resistance decreases with the amount of deposited solution.	[9, 10]

V) Numerical simulation of current distribution in percolative film with strain

To visualize the strain-induced changes to the percolative films, we carry out numerical simulations for the percolative film. In the simulation model, individual links consists of certain number of resistance nodes and the resistance between links depends on the amount of overlap between them. This process produces a large resistance network with several thousand connections. Applying Kirchoff's laws, we can obtain the overall resistance of the film. By comparing the change of overall resistance upon displacement of the links, strain-induced changes to the percolation can be demonstrated. Thus, the current within and across conductive links can be obtained and the distribution of currents across the sample is displayed in Figure 2(a). As shown in the Figure 2(a), the strain leads to fewer pathways for carrier transport, leading to higher current densities in critical connections but an overall increase in film resistance. For the two films in Figure2(a), the overall resistance of unstrained film is 100Ω while the overall resistance of strained film is 293Ω.

References

1. W. Bauhofer and J. Z. Kovacs, *Composites Science & Technology*, 2009, **69**, 1486-1498.
2. S. De, P. J. King, P. E. Lyons, U. Khan and J. N. Coleman, *Acs Nano*, 2010, **4**, 7064-7072.
3. P. E. Lyons, S. De, J. Elias, M. Schamel, L. Philippe, A. T. Bellew, J. J. Boland and J. N. Coleman, *The Journal of Physical Chemistry Letters*, 2011, **2**, 3058-3062.
4. A. A. Saberi, *Physics Reports*, 2015, **578**, 1-32.
5. S. Sorel, P. E. Lyons, S. De, J. C. Dickerson and J. N. Coleman, *Nanotechnology*, 2012, **23**, 185201.
6. D. Stauffer and A. Aharony, *Introduction to percolation theory: revised second edition*, CRC press, 2014.
7. S. De, P. J. King, M. Lotya, A. O'Neill, E. M. Doherty, Y. Hernandez, G. S. Duesberg and J. N. Coleman, *Small*, 2010, **6**, 458-464.
8. N. McEvoy, N. Peltekis, S. Kumar, E. Rezvani, H. Nolan, G. P. Keeley, W. J. Blau and G. S. Duesberg, *Carbon*, 2012, **50**, 1216-1226.
9. Z. Chen, T. Ming, M. M. Goulamaly, H. Yao, D. Nezich, M. Hempel, M. Hofmann and J. Kong, *Advanced Functional Materials*, 2016, **26**, 5061-5067.
10. M. Hempel, D. Nezich, J. Kong and M. Hofmann, *Nano Letters*, 2012, **12**, 5714-5718.
11. S. Stassi, V. Cauda, G. Canavese and C. F. Pirri, *Sensors*, 2014, **14**, 5296-5332.
12. D. Ponnamma, Q. Guo, I. Krupa, M. A. Almaadeed, K. T. V, S. Thomas and K. K. Sadasivuni, *Physical Chemistry Chemical Physics*, 2015, **17**, 3954.
13. L. Chen, G. Chen and L. Lu, *Adv. Funct. Mater.*, 2007, **17**, 898-904.
14. G. T. Pham, Y. B. Park, Z. Liang, C. Zhang and B. Wang, *Composites Part B Engineering*, 2008, **39**, 209-216.
15. T. D. Gupta, T. Gacoin and A. C. H. Rowe, *Adv. Funct. Mater.*, 2014, **24**, 4522-4527.